Published March 14, 2014

Characterizing Compaction Variability with an Electromagnetic Induction Sensor in a Puddled Paddy Rice Field

M. M. Islam*
E. Meerschman
T. Saey
P. De Smedt
E. Van De Vijver
S. Delefortrie
M. Van Meirvenne
Dep. of Soil Management
Faculty of Bioscience Engineering
Ghent Univ.
Coupure 653
9000 Gent, Belgium

Paddy rice (*Oryza sativa* L.) fields are repeatedly puddled at water saturation to loosen the top soil and to form a uniformly compacted plow pan required to reduce losses of water and nutrients. In paddy growing conditions however, the non-invasive detection of compaction variation within the plow pan layer is challenging. This paper evaluates a proximal soil sensing based methodology to identify areas compacted by different intensities of puddling to support precise land preparation of paddy rice fields. Therefore, a 1.6-ha alluvial paddy field of silt loam texture (Aeric Haplaquepts) located in the Brahmaputra floodplain of Bangladesh was selected. Three areas within the field were variably puddled and characterized by soil properties and soil apparent electrical conductivity (EC_a). The Floating Soil Sensing System (FLoSSY) employing the EM38 electromagnetic induction sensor was used to record the EC_a of the soil for each of the puddling intensities. The effects of plow pan compaction on water percolation losses and paddy yield were assessed. The results show that the variably puddled areas had significant differences in soil bulk density which was linked to the soil penetration resistance. Spatial comparison of EC_a data sets showed that the EC_a values increased systematically under increased puddling. Sufficient soil compaction could be identified when percolation losses were significantly the lowest and paddy yield was significantly the highest. It was concluded that a non-invasive EC_a survey using electromagnetic induction based soil sensing allowed the detection of soil heterogeneity linked to soil compaction caused by puddling, which offers an interesting potential for precision puddling and land preparation in paddy rice fields.

Abbreviations: EC_a, apparent electrical conductivity; Exp-1, Experiment 1; Exp-2, Experiment 2; Exp-3, Experiment 3; FLoSSY, The floating soil sensing system; OK, ordinary kriging; PR, penetration resistence; SK, simple kriging; SKlm, simple kriging with varying local means.

The specialized land preparation practice of puddling requires the paddy rice farmers to work the soil at water saturation. Puddling helps to control weeds, to ease the transplantation of rice seedlings and to maintain a uniform water depth over the field (Mohanty et al., 2004). Effects of puddling include a decrease in total porosity and a marked redistribution of soil pores as a result of rearrangement of soil particles (De Datta, 1981; Gajri et al., 1999). Most macropores transmitting water are eliminated and the remaining macropores are partially or completely filled by dispersed finer soil particles (Kukal and Aggarwal, 2003). This results in a drastic reduction in water and nutrient losses caused by deep percolation below the rooting zone (McDonald et al., 2006). Limiting percolation

Soil Sci. Soc. Am. J. 78:579–588
doi:10.2136/sssaj2013.07.0289
Received 19 July 2013
*Corresponding author (mohammadmonirul.islam@ugent.be)

losses and maintaining a flooded condition is crucial to wet paddy cultivation (Kukal and Sidhu, 2004). Standing water in paddy fields not only inhibits further weed infestation during crop development but also increases crop-water availability in periods of limited rainfall. Water availability to the plants increases as percolation rate decreases due to reduction in the hydraulic conductivity of the puddled soil layer (Sharma and De Datta, 1985). Thus, puddling remains as a unique method of land preparation for irrigated and lowland paddy rice cultivation.

During land preparation the puddled layer gradually becomes stratified into a standing water layer and a loose water saturated soil layer. Beneath these two, a relatively impermeable dense soil layer known as the plow pan is formed. The formation of a paddy field plow pan requires subsoil compaction which involves repeated plowing at the same depth using typical paddy field cultivators (De Datta, 1981). A paddy field is optimally puddled when the saturated loose soil layer provides a better physical condition for plant root growth, while the plow pan beneath is compacted enough to restrict water and nutrient losses beyond the rooting depth. However, the degree of compaction of the plow pan is mainly influenced by puddling (De Datta, 1981). A poorly compacted plow pan makes a paddy field prone to nutrient losses through leaching and water losses through percolation. On the other hand, too many puddlings may incur unnecessary waste of water and energy inputs and can have severe consequences in water scarce regions.

In the absence of specific guidance, the intensity of a puddling operation by the paddy farmer usually depends on the availability of water resources (Playán et al., 2008). Despite being capital and energy intensive, paddy farmers commonly opt for high intensity puddling to attain a presumably homogeneous and sufficiently compacted plow pan. This happens because the detection of compaction during a puddling practice is not readily available. First, flooded conditions make the paddy fields inaccessible for direct observations (Islam et al., 2012) and second, difficult for indirect measurements (Hemmat and Adamchuk, 2008). Furthermore, the standing water layer on top of the saturated soil layer obscures the extraction of soil information using technologies like remote sensing systems (Islam et al., 2011). However, obtaining information on soil compaction during puddling would be beneficial to guide the farmers. For this, acquisition of detailed and geo-referenced soil information, aiming at the adjustment of puddling induced soil compaction needs to be considered. In this regard, obtaining high resolution soil information using proximal sensing systems can serve as a basis for identifying compaction variation and managing soil resources.

Proximal soil sensing using an electromagnetic induction (EMI) based sensor provides the opportunity to measure the soil EC_a information while avoiding direct physical contact with the measured soil. In the case of non-saline soils, interpretation of the EC_a measurements explains the underlying variation in soil physical properties (Sudduth et al., 1997) such as texture (Saey et al., 2009) and compaction (Brevik and Fenton, 2004); moisture (Brevik et al., 2006), bulk density or pore volume (Rhoades et al., 1999), and depth to clay layer (Saey et al., 2009a). Thus, mobile EC_a surveys complemented with a GPS allow spatial monitoring of soil properties which are relevant for crop growth. Because the traditionally used EC_a surveying systems used in unsaturated field conditions are not applicable as such in flooded paddy fields, a proximal floating soil sensing system suited to operate on flooded fields was designed (Islam and Van Meirvenne, 2011). The system offers the advantage of strongly reducing the effect of moisture differences on the EMI signal (Islam et al., 2012). Therefore, the EC_a measurements under flooded condition offer the possibility of reflecting the dynamic soil physical changes that take place during puddling.

The purpose of this paper is to assess the applicability of a proximal sensing system to detect the compaction variability at a field scale. The objective is three-fold: (i) characterization of puddling induced soil compaction in terms of soil attributes, (ii) spatial characterization of differentially compacted areas using high resolution soil EC_a measurements, and (iii) evaluating these compacted areas in terms of water percolation and paddy yield.

MATERIALS AND METHODS

Study Site

A 1.6-ha paddy field located at the Bangladesh Agricultural University, Mymensingh in Bangladesh was selected for the 3-yr study (2009–2011). The field, with central coordinates 24.720038°N and 90.427007°E, lies about 8 m above sea level. It has a traditional paddy cultivation history of more than 45 yr, including puddling of soil as a land preparation practice before crop planting. The soil of the field was developed on the alluvial deposits of the river Brahmaputra and generally consists of fine sand to silty material (Aeric Haplaquepts; Brammer, 1996). A reconnaissance soil survey reported these alluvial floodplain soils as non-saline (Brammer, 1981). The study region has a tropical monsoon climate and receives about 1887 mm of precipitation between May and September. Precipitation is approx. 15.2 ± 1.6 mm between November and January.

Compaction Experiments

The experimental strategy contained different stages. First, the field was brought to an evenly tilled condition. Next, soil compaction development was introduced through gradually increasing the intensity of puddling. Therefore, three experiments were performed. Figure 1 shows a schematic layout of the field for the three experiments.

Experiment-1 (Exp-1) was initiated in October 2009 and the same treatments were applied on the entire field. First, a dry deep tillage with a 35-HP tractor operated disc plow was used to remove previous tillage influences and to reach an equally tilled condition. Second, harrowing once with a tine cultivator was followed by flooding the entire field (flood irrigation) to a height of ~0.15 m. No puddling (P0) was done before paddy planting.

Experiment-2 (Exp-2) was conducted in September 2010 for which the field was first harrowed twice at weekly intervals.

Then it was flooded to ~0.15-m water height and made ready for puddling, using repeated passes of a 12-HP power tiller. A power tiller is a semiautomatic manually operated vehicle equipped with L-shaped tilling blades and cage wheels to conduct puddling operations in wet paddy fields. The paddy field was marked into three areas to receive three puddling intensity treatments. Thus, starting from the west and moving toward the east, three consecutive areas of ~90 m × 50 m each were fixed. The three puddling intensities applied were one puddling (Exp-2P1), two puddling (Exp-2P2), and three puddling (Exp-2P3) for the three areas, respectively.

Experiment-3 (Exp-3) started in October 2010 and three puddling intensities were applied for the same three areas of Exp-2 having ~0.15 m water height. The puddling intensity treatments were two (Exp-3P2), four (Exp-3P4), and six (Exp-3P6), respectively. So for the same areas, the puddling intensities of Exp-2 were doubled in Exp-3.

Soil Sampling and Analysis

In September 2009, soil samples were collected at three depth intervals of 0 to 0.15, 0.15 to 0.30, and 0.30 to 0.45 m. Within 1 m^2 at each location, three replicated soil samples were taken and pooled.

After draining the field was sampled again in April 2011 when the soil moisture content was about field capacity. To ensure equal field coverage, 54 locations were identified according to a regular grid of 16 m by 15 m. Three replicates of undisturbed soil samples were collected within 1 m^2 of every location for three depth intervals: 0 to 0.15, 0.15 to 0.30, and 0.30 to 0.45 m. The known volume of the sampling core (0.75 L) and the oven dried (105°C) weight of the soil samples were used to calculate the average soil bulk density at each location. Next, the replicated soil samples were pooled and the three major textural fractions (clay: 0–2 μm, silt: 2–50 μm, and sand: 50–2000 μm) were analyzed using the conventional sieve-pipette method, while organic carbon (OC) was determined by the Walkley and Black method (Walkley and Black (1934).

Within 1 m^2 of the 54 sampling locations, soil penetration resistance (PR) was measured by a SC900 soil compaction meter (Spectrum Technologies Inc., Illinois). The meter has a 30° conical probe with 12.82-mm diam. ASAE standard small tip and takes compaction readings to a depth of 0.45 m at 0.025-m increments using an ultrasonic depth sensor. Penetration resistance was measured by an internal load cell and recorded in a data logger in kilopascals (kPa). At each location three replicated readings were taken and averaged.

The Floating Sensing System

To acquire high resolution soil data on flooded paddy field conditions, a mobile soil sensing system called FloSSy was used. In FloSSy, a non-invasive EMI sensor was mounted because these sensors do not require a direct ground contact to acquire soil information. Here, the EM38 sensor (Geonics Limited, Canada) was used, which is suitable for a floating sensing system due to its light-weight (about 3.5 kg) and small physical dimensions (1.05 m × 0.16 m × 0.05 m). The instrument records the apparent conductivity of soil at a particular location by measuring the apparent flow of current through a soil volume going from a transmitter to a receiver. The transmitting and receiving coil spacing of the EM38 sensor is 1 m. Operating principles, depth weighting functions, and technical details of the sensor can be found in McNeill (1980). Operating the sensor in the vertical orientation, as is done in this study, results in a depth of influence of about 1.5 m, representing 70% of its accumulated depth response under homogeneous soil conditions. This orientation receives a dominant influence from the 0.3- to 0.6-m soil layers. Hence, with a standing water depth of about 0.15 m in the paddy field, influence of the soil material beneath the water layer could be measured. It is worthwhile mentioning that the horizontal orientation of the sensor would receive a strong influence from the standing water layer making it inappropriate for paddy fields.

In the FloSSy, the EM38 is contained in a waterproof housing placed on a wooden raft (Fig. 2). The raft is equipped with a GPS receiver with differential correction (a pass to pass accuracy of ± 0.20 m), so that its position indicates the center of the sensor.

The raft trailed the power tiller at a distance of approximately 1.5 m. Geo-referenced EC_a data acquired by the system were logged and processed in situ in a field laptop. More details on FloSSy can be found in Islam and Van Meirvenne (2011).

Apparent Electrical Conductivity Survey and Data Processing

To have EC_a information as a function of compaction, the inundated field was surveyed three times for the three experiments, in October 2009 (for Exp-1), in September 2010 (for Exp-2), and 1 mo later in October 2010 (for Exp-3). During all surveys, measurements were taken along parallel lines with a spatial resolution of 0.3 m × 0.7 m. A temperature sensor pushed

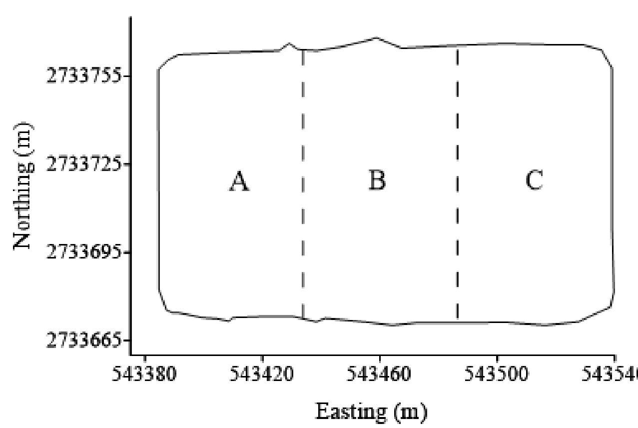

Fig. 1. Experimental layout of the field in three areas indicated as A, B, and C. Experiment 1 (Exp-1) consisted of the P0 (no puddling) treatment in all three areas; Experiment 2 (Exp-2) consisted of Exp-2P1 (one puddling), Exp-2P2 (two puddlings) and Exp-2P3 (three puddlings) in A, B, and C, respectively; Experiment 3 (Exp-3) consisted of Exp-3P2 (two puddlings), Exp-3P4 (four puddlings) and Exp-3P6 (six puddlings) in A, B, and C, respectively; dashed lines indicate treatment boundaries.

Fig. 2. The Floating Soil Sensing System (FloSSy) during field measurement of apparent electrical conductivity (EC_a). The different components are indicated as: (i) laptop, (ii) GPS, (iii) water proof sensor housing, (iv) floating platform, and (v) the power tiller.

into the ground up to a depth of 0.25 m below the surface recorded the soil temperature during the EC_a surveys. It remained stable during the survey at 30°C. Obtained EC_a measurements were post-corrected for instrumental drift according to the deviation from an initial diagonal measurement across the field. Resulting data were standardized to a reference temperature of 25°C (Sheets and Hendrickx, 1995):

$$EC_{a_{25}} = EC_{a_{obs}} \left(0.4470 + 1.4034.e^{-T/26.815}\right) \quad [1]$$

with $EC_{a_{25}}$ the standardized EC_a values at 25°C and $EC_{a_{obs}}$ the observed EC_a values at soil temperature T (°C). These standardized EC_a values are used in the following part of this paper.

Geostatistical Interpolation

The three EC_a measurement data sets were interpolated to a regular grid with a 0.5 m × 0.5 m resolution using kriging. Kriging is a family of geostatistical techniques to estimate the value of a random variable Z at any unsampled location $\mathbf{X}_0$, that is, $Z^*(\mathbf{X}_0)$, using a weighted linear combination of $n(\mathbf{X}_0)$ observations within a predefined neighborhood around $\mathbf{X}_0$. The general kriging equation is (Goovaerts, 1997):

$$Z^*(\mathbf{x}_0) - m(\mathbf{x}_0) = \sum_{\alpha=1}^{n(\mathbf{x}_0)} \lambda_\alpha \left[Z(\mathbf{x}_\alpha) - m(\mathbf{x}_\alpha)\right] \quad [2]$$

with λ_α the assigned weights, $m(\mathbf{X}_0)$ the expected value of random variable $Z(\mathbf{X}_0)$ and $m(\mathbf{X}_\alpha)$ the expected value of random variable $Z(\mathbf{X}_\alpha)$. The weights are assigned by solving a kriging system which minimizes the estimation variance under the constraint of unbiasness of the estimator.

For all types of kriging, the kriging system relies on the variogram model. This is a model for the spatial structure of Z and is obtained by fitting a continuous function to the experimental variogram, calculated as:

$$\gamma(\mathbf{h}) = \frac{1}{2N(\mathbf{h})} \sum_{\alpha=1}^{N(\mathbf{h})} \left\{z(\mathbf{x}_\alpha + \mathbf{h}) - z(\mathbf{x}_\alpha)\right\}^2 \quad [3]$$

with $\gamma(\mathbf{h})$ the variogram for a distance vector (lag) $\mathbf{h}$ between observations $z(\mathbf{x}_\alpha + \mathbf{h})$ and $z(\mathbf{x}_\alpha)$, and $N(\mathbf{h})$ the number of pairs separated by $\mathbf{h}$. Typically, $\gamma(\mathbf{h})$ increases with increasing lag distances $\mathbf{h}$. Only a limited number of permissible models can be fitted to the experimental variogram. More details about the kriging system and variogram modeling can be found in Goovaerts (1997) and Webster and Oliver (2007).

Although all kriging variants are based on the general kriging equation (Eq. [2]) and the variogram model, three variants can be distinguished according to the model considered for $m(\mathbf{x})$: simple kriging (SK), ordinary kriging (OK), and simple kriging with varying local means (SKlm).

Simple kriging (SK) assumes that $m(\mathbf{x})$ is globally stationary, so it simply becomes m, and that is it is known a priori. Therefore, SK works on the residuals and its kriging estimator is

$$Z^*_{SK}(\mathbf{x}_0) = m + \sum_{\alpha=1}^{n(\mathbf{x}_0)} \lambda_\alpha R(\mathbf{x}_\alpha) \quad [4]$$

with $R(\mathbf{x}_\alpha) = Z(\mathbf{x}_\alpha) - m$. Hence, SK first subtracts the known global mean m from all observations, then interpolates the residuals using the SK kriging system, and finally adds back m to all estimations. Note that the SK assumptions about $m(\mathbf{x})$ are severe and difficult to verify.

Ordinary kriging (OK) is a second kriging type which has more relaxed assumptions about $m(\mathbf{x})$: it assumes that $m(\mathbf{x})$ is locally stationary and that it is unknown. This means that $m(\mathbf{x})$ is constant within the predefined neighborhood around $\mathbf{x}_0$, implying that $m(\mathbf{x}_0)$ and $m(\mathbf{x}_\alpha)$ are equal. This results in the OK estimator:

$$Z^*_{OK}(\mathbf{x}_0) = \sum_{\alpha=1}^{n(\mathbf{x}_0)} \lambda_\alpha Z(\mathbf{x}_\alpha) \quad \text{with} \quad \sum_{\alpha=1}^{n(\mathbf{x}_0)} \lambda_\alpha = 1 \quad [5]$$

The sum of the weights must be equal to one to assure unbiasedness of the estimator. In the absence of a clear spatial trend, the OK assumptions of local stationarity can be accepted, making OK an often used interpolation method.

In the presence of a clear spatial trend, in other words when $m(\mathbf{x})$ is non-stationary, SKlm could be applied. In SKlm the global mean m of SK is replaced by a varying local mean $m(\mathbf{x})$ which is modeled for the entire study area, leading to the following kriging equation

$$Z^*_{SKlm}(\mathbf{x}_0) = m(\mathbf{x}_0) + \sum_{\alpha=1}^{n(\mathbf{x}_0)} \lambda_\alpha R(\mathbf{x}_\alpha) \quad [6]$$

with $R(\mathbf{x}_\alpha) = Z(\mathbf{x}_\alpha) - m(\mathbf{x}_\alpha)$, that is, the residuals at the observed locations. Similar to SK, SKlm first subtracts the varying local mean or spatial trend $m(\mathbf{x})$ from all observations.

Since the mean of the residuals $R(\mathbf{x}_\alpha)$ can be considered as globally stationary and it is equal to zero. The residuals are interpolated with the SK kriging system. Finally, $m(\mathbf{x})$ is added back to all estimations. In SKlm the variogram of the residuals is calculated and modeled. For both variogram analysis and kriging the mapping software Surfer 11.0 was used (Golden Software Inc., Golden, CO).

Table 1. Population parameters of soil textural fractions and OC (organic carbon) at three soil depths; number of samples (n) = 54.

Soil depth		OC	Sand	Silt	Clay	Soil texture class
m		%		g kg^{-1}		
0–0.15	Minimum	2.1	240	520	150	
	Maximum	2.5	330	580	190	
	Mean	2.3	279	545	176	Silt loam
	SD	0.12	24.7	21.1	15.6	
0.15–0.30	Minimum	1.6	230	530	130	
	Maximum	2.4	320	620	180	
	Mean	1.9	263	580	157	Silt loam
	SD	0.27	29.6	32.0	15.0	
0.30–0.45	Minimum	1.9	400	360	100	
	Maximum	2.4	510	490	140	
	Mean	2.2	442	438	120	Loam
	SD	0.17	28.9	32.2	11.6	

Water Percolation and Crop Yield Measurements

Water percolation was measured in November 2010 for Exp-3 to observe the effect of compaction on water losses. At the 54 soil sampling locations readings were taken periodically three times within 1 m^2 with a double ring infiltrometer (0.30 m inner ring diameter and 0.45 m outer ring). The decrease in water level in the inner ring as a function of time was measured. Measurements continued for 3 d as the water inside the inner ring approached a stable level. Percolation rates were determined from data on ring water levels and evaporation from an open pan located inside the field and surrounded by paddy rice plants.

At each of the 54 sampling locations the paddy grain yield was determined for Exp-1 and Exp-3. The crops were planted in October 2009 and 2010 and harvested in March 2010 and 2011, respectively. Planting density, intercultural practices, fertilizer and irrigation water inputs were equally applied to the crop over the study years. So, evaluation of crop performance for the two experiments involving no compaction and maximal compaction was made possible. At maturity, the paddy grain of 1 m^2 was manually harvested. The weight of the harvested fresh grains was measured, adjusted to a moisture content of 14% (International Seed Testing Association, 2011) and expressed in Mg ha^{-1}.

RESULTS AND DISCUSSION

Soil Texture, Organic Carbon, Bulk Density and Penetration Resistance

The field was characterized at 54 sampling locations with respect to soil texture, bulk density and penetration resistance (PR). Table 1 shows the population parameters of soil texture and OC analysis of the field observed at three depth intervals.

On average the soil (0–0.30 m) has a silt loam texture [United States Department of Agriculture (USDA) texture triangle] with a predominant silt fraction (above 50%). There is a small change at depth (0.30–0.45 m), where the texture becomes loamy. Small standard deviation (SD) values for the textural fractions within each depth interval were found. The mean OC content of the field was not very high (2.3% within 0–0.15 m) and also did not differ much with depth increment. With low values of SD (maximum 0.27, within 0.15–0.30 m), the OC content exhibited a limited spatial variability in the distribution of soil organic matter.

To investigate the link between compaction and soil bulk density, the 54 observations of bulk density at the three depth intervals were grouped according to the puddling intensities of Exp-2 and Exp-3. Table 2 gives the descriptive statistics together with a statistical comparison of the mean bulk density values.

For all three soil depth intervals, the mean bulk density values were generally low within the 0- to 0.15-m soil layer (ranged between 1.26 and 1.55 Mg m^{-3}) and generally high within the 0.15- to 0.30-m soil layer (ranged between 1.47 and 1.73 Mg m^{-3}). Mean values within the 0.30- to 0.45-m soil depth were intermediary (ranged between 1.46 and 1.50 Mg m^{-3}). Within 0 to 0.15 m, Exp-2P1 had the largest mean bulk density (1.55 Mg m^{-3}). This was significantly different from the other

Table 2. Descriptive statistics and mean comparison of soil bulk density (Mg m^{-3}) between puddling intensities of Experiment 2 (Exp-2): Exp-2P1 = one puddling, Exp-2P2 = two puddling and Exp-2P3 = three puddling; Experiment 3 (Exp-3): Exp-3P2 = two puddling, Exp-3P4 = four puddling, and Exp-3P6 = six puddling; n = number of samples, SD = standard deviation.

Soil depth, m	Puddling intensity	N	Soil bulk density (Mg m^{-3}) Minimum	Maximum	Mean†	SD
0–0.15	Exp-2P1	18	1.29	1.70	1.55_a	0.13
	Exp-2P2	18	1.28	1.42	1.37_b	0.05
	Exp-2P3	18	1.27	1.41	1.32_c	0.04
	Exp-3P2	18	1.29	1.42	1.37_b	0.05
	Exp-3P4	18	1.20	1.35	1.26_d	0.04
	Exp-3P6	18	1.17	1.36	1.26_d	0.05
0.15–0.30	Exp-2P1	18	1.35	1.67	1.47_a	0.10
	Exp-2P2	18	1.42	1.76	1.55_b	0.10
	Exp-2P3	18	1.51	1.77	1.64_c	0.05
	Exp-3P2	18	1.42	1.76	1.55_b	0.10
	Exp-3P4	18	1.60	1.78	1.73_d	0.04
	Exp-3P6	18	1.61	1.79	1.72_d	0.05
0.30–0.45	Exp-2P1	18	1.42	1.54	1.46	0.05
	Exp-2P2	18	1.42	1.53	1.48	0.04
	Exp-2P3	18	1.44	1.54	1.48	0.04
	Exp-3P2	18	1.43	1.54	1.48	0.05
	Exp-3P4	18	1.44	1.59	1.49	0.05
	Exp-3P6	18	1.45	1.60	1.50	0.05

†Within a soil depth interval, means followed by the same letter or without a letter do not differ significantly (p = 0.05) according to Fisher's least significant difference test.

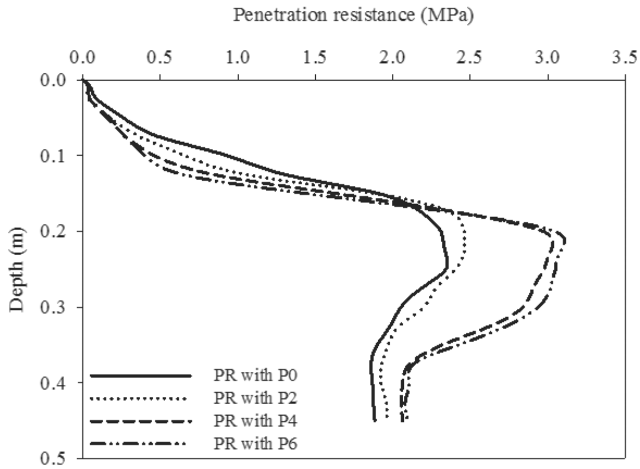

Fig. 3. Penetration resistance (PR) at different depths as a function of puddling intensity treatments of Exp-1: P0 = no puddling and Exp-3: P2 = two puddling, P4 = four puddling and P6 = six puddling.

two puddling intensities of Exp-2 and all the three intensities of Exp-3, where the bulk density values were lower. The general decrease in bulk density with increasing puddling intensity was caused by the loosening effect of puddling, which implies a compaction reduction. So, bulk density in the 0- to 0.15-m interval followed the opposite trend of the puddling intensity, that is, the higher the puddling intensity, the lower the bulk density. The bulk density values observed for the 0.15- to 0.30-m depth interval were higher because the plow pan formation took place at this depth. In other studies, the bulk density of a sandy loam soil layer at 0.15- to 0.20-m depth has also been found to increase with an increase in puddling (e.g., Kukal and Aggarwal, 2003). However, in this study a large variation in bulk density values was observed within the 0.15- to 0.30-m soil layer of Exp-3. This was indicated by a larger range of SD values (0.04 to 0.10 Mg m^{-3}) compared with the other two soil layers. This large SD value of 0.10 Mg m^{-3} indicated that puddling at two intensities still created large variation, and therefore, was not sufficient to form a plow pan having homogeneous soil compaction. Compaction was increased in Exp-3P4 and Exp3-P6. Consequently, soil bulk density in the 0.15- to 0.30-m layer increased significantly as compared with the same areas of Exp-2 while SD values decreased, indicating a better compacted plow pan with a rather homogeneous coverage. This indicates the link between increased puddling intensity and plow pan compaction. The deeper soil layer (0.30–0.45 m) was probably uninfluenced by puddling and thereby did not show any significant difference for the individual puddling treatments. This is supported by Fig. 3 which illustrates the PR measurements as a result of increased puddling intensity.

Soil resistance to penetration was minimal within the plow layer (0–0.15 m) because puddling could loosen the soil up to this depth. The soil of this layer became softer with increased puddling intensity as aggregates were broken down due to the mechanical action (Mousavi et al., 2009), thereby decreasing soil PR. Beneath the plow layer, PR increased with an increase in puddling intensity and reached a value above 3.0 MPa in Exp-3P6. It is clear from Fig. 3 that the resistance of around 3.0 MPa was observed within the 0.15- to 0.30-m soil depth; the same depth where bulk density was high (Table 2). The results were similar in Exp-2 (data not shown). Kukal and Aggarwal (2003) also reported significantly higher soil PR after puddling, because of increased compaction within the plow pan layer. The deep soil layer (0.30–0.45 m) was least influenced by puddling and remained relatively stable to offer an intermediary level of resistance.

Table 3. Population parameters of apparent electrical conductivity (EC_a) meaurements of the three surveys across the paddy field; EC_a of Experiament 1 (Exp-1): no puddling treatment; EC_a of Experimental 2 (Exp-2) with one, two, and three puddling treatments; EC_a of Experiment 3 (Exp-3) with two, four, and six puddling treatments; *n* = number of samples.

EC_a survey	EC_a				
	n	Minimum	Maximum	Mean	Variance
		———————mS m^{-1}	———————		(mS $m^{-1})^2$
Exp-1	54 234	46	56	50.4	3.2
Exp-2	54 204	50	65	58.6	13.1
Exp-3	54 239	53	67	61.1	13.7

Apparent Electrical Conductivity Survey

Table 3 shows the population parameters of the EC_a measurements for the three surveys. The mean of EC_a of Exp-3 (61.1 mS m^{-1}) was higher than those of Exp-2 (58.6 mS m^{-1}) and Exp-1 (50.4 mS m^{-1}). A difference in the variance was also observed: 3.2 (mS $m^{-1})^2$ for Exp-1, 13.1 (mS $m^{-1})^2$ for Exp-2, and 13.7 (mS $m^{-1})^2$ for Exp-3. This indicated an increase of EC_a variability when the puddling intensity was also increased. As the surveys were conducted by the same sensing system in flooded conditions, the general increase in EC_a for Exp-2 and Exp-3 can be attributed to changes in soil condition.

Figure 4 shows the box plots of EC_a for the puddling intensities for the three experiments. Figure 4a clearly shows that the mean EC_a of Exp-1 was stationary for the three areas of the paddy field receiving the same puddling treatment P0. In Exp-2 (Fig. 4b) the expected values started approaching to non-stationarity which became clearly non-stationary in Exp-3 (Fig. 4c). So, the three areas with different puddling intensity treatments: Exp-3P2, Exp-3P4, and Exp-3P6 were transformed to have clearly different local means (Exp-3). Thus, the presence of spatial trend caused by soil compaction was evident.

We chose OK to interpolate the EC_a data from the Exp-1 and SKlm to interpolate the EC_a data from Exp-2 and Exp-3, because there was a clear spatial trend for the last two. To model the variogram, these two survey data sets were stratified per puddling intensity and the local mean values were subtracted from observations in the respective stratum to obtain residuals. Figure 5 shows the experimental variograms and the fitted exponential models (Goovaerts, 1997) for the EC_a data set of Exp-1 and pooled residuals of EC_a of Exp-2 and Exp-3. The spatial continuity for the EC_a data set of Exp-1 (Fig. 5a) had a range (*a*) of 29 m which was higher than those of the residual data sets of Exp-2 (Fig. 5b) and Exp-3 (Fig. 5c). Both the structured part of the spatial variation and the maximal extend of spatial

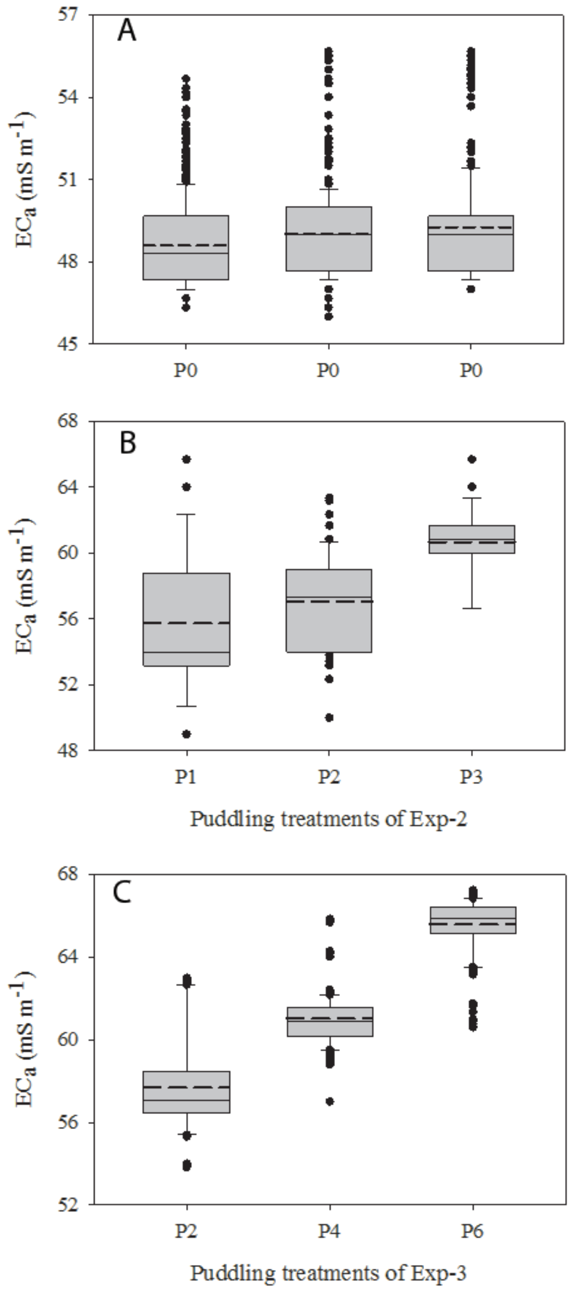

Fig. 4. Box plots of apparent electrical conductivity (EC_a; mS m^{-1}) values of the paddy field in three areas: (a) EC_a of Experiment 1 (Exp-1) with no puddling (P0) in all three areas; (b) EC_a of Experiment 2 (Exp-2) with P1 (one puddling), P2 (two puddling), and P3 (three puddling); and (c) EC_a of Experiment 3 (Exp-3) with P2 (two puddling), P4 (four puddling), and P6 (six puddling). The top and bottom of the boxes are the first and third quartiles, respectively. The length of the box thus represents the interquartile range. The solid line through the middle of each box represents the median and dashed line the mean. The vertical bars show the extent between the 10th and 90th percentiles and solid circles represent values outside the 10th and 90th percentiles.

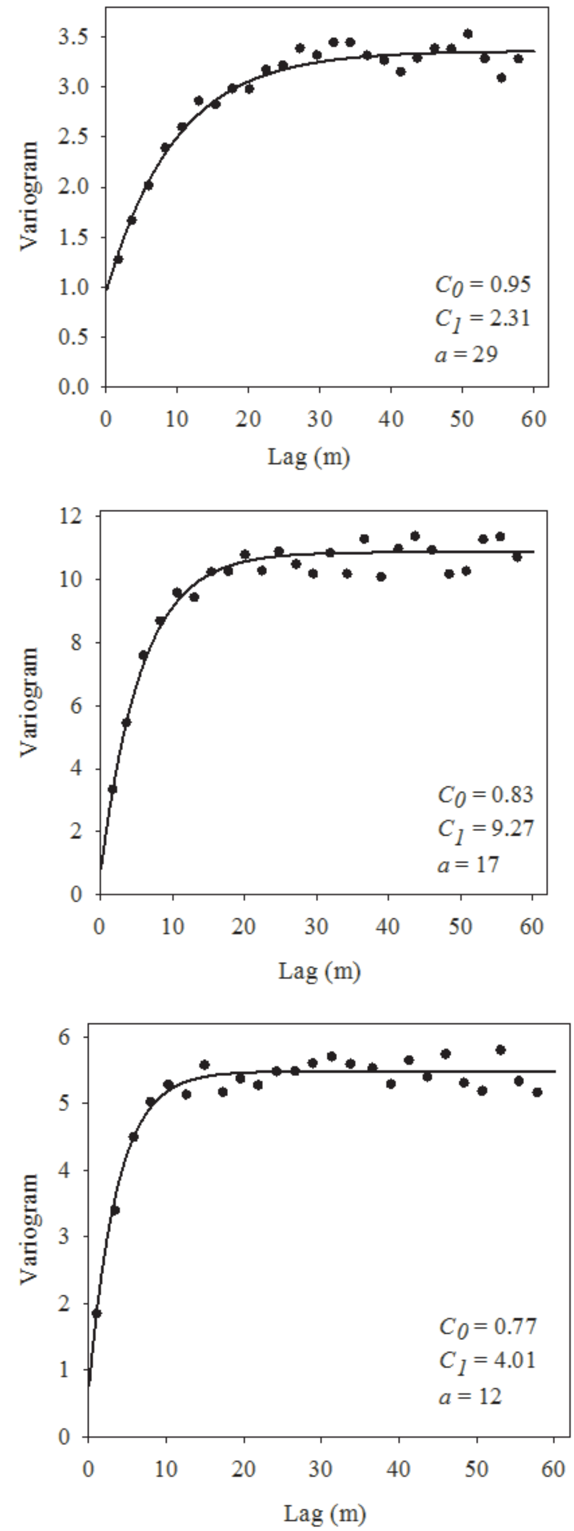

Fig. 5. The experimental variograms (dots) and the exponential models (line) of three data sets: (a) apparent electrical conductivity (EC_a) of Experiment 1 (Exp-1), (b) pooled residuals of EC_a of Experiment 2 (Exp-2), and (c) pooled residuals of EC_a of Experiment 3 (Exp-3). The parameters of the fitted variogram models are also given: C_0 (nugget), C_1 (sill), and a (range) expressed in meters.

relation decreased as soil compaction increased in Exp-3P4 and Exp-3P6. This was indicated by smaller C_1 and a values of the EC_a residuals in Exp-3P4 and Exp-3P6.

Figure 6 shows the EC_a measurements of the field: EC_a of Exp-1 interpolated with OK, and EC_a of Exp-2 and Exp-3 interpolated with SKlm. However, stratifying the EC_a data of Exp-2 (according to Exp-2P1, Exp-2P2, and Exp-2P3) and Exp-3 (according to Exp-3P2, Exp-3P4, and Exp-3P6) could result in too few measurements within each stratum for variogram modeling and this technique could induce artifacts along the boundaries (Meul and Van Meirvenne, 2003). With

SKlm the effect of the differences in mean was removed and the residuals were pooled yielding sufficient data for variogram calculation and modeling.

The EC_a map of Exp-1 in Fig. 6a shows patterns of fluctuating EC_a values across the field. It can be seen that some patchy areas of high EC_a values occurred within the field, especially at the middle of the southern border. Occurrence of these high EC_a values was investigated by field observation and could be attributed to few large soil clods which appeared after disc plowing. Apart from that, the field did not have a large EC_a variation before puddling for Exp-2. After puddling however, the EC_a map in Fig. 6b for Exp-2 shows a trend of increasing EC_a values from west to the east side of the field. This is the same direction toward which puddling increased in Exp-2P2 and Exp-2P3 over Exp-2P1 (for Exp-2). This spatial trend of increasing EC_a values was even better captured during the EC_a survey of Exp-3 and is mapped in Fig. 6c. This map clearly shows the three distinct areas within the field which sequentially received Exp-3P2, Exp-3P4, and Exp-3P6, thereby an increasingly higher puddling intensity. Thus, the connection between EC_a as a representation of plow pan compaction variation caused by puddling was evident.

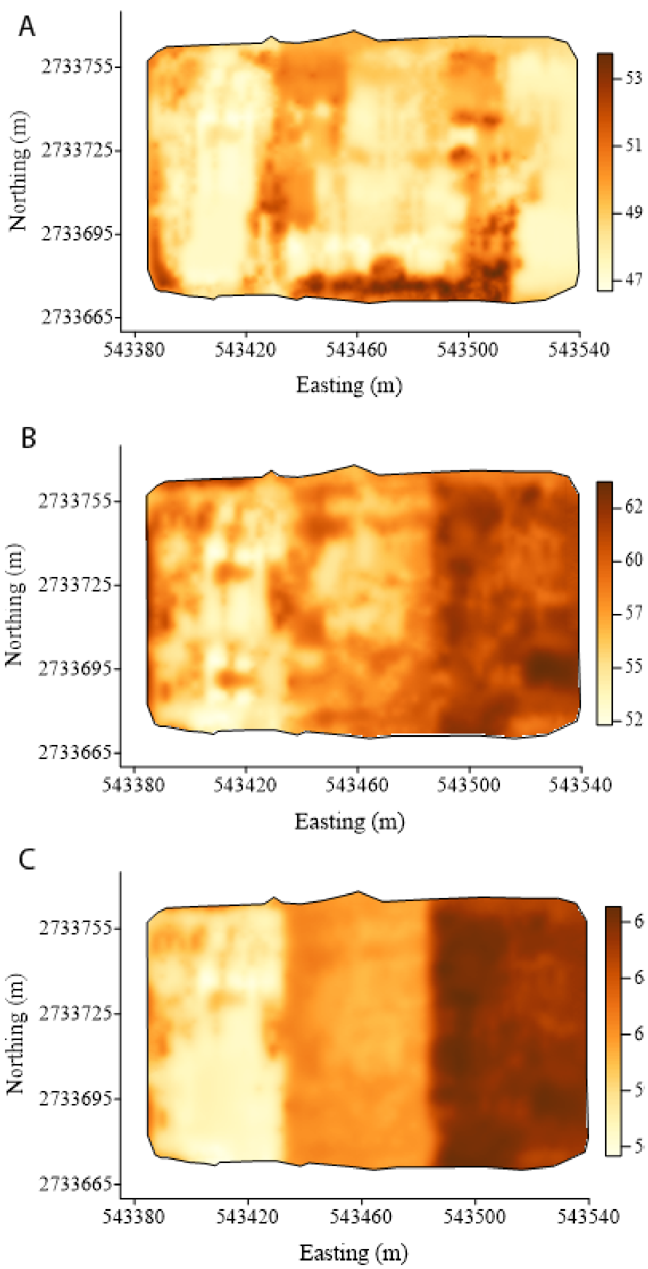

Fig. 6. The interpolated apparent electrical conductivity (EC_a) of the paddy field: (a) EC_a (mS m^{-1}) of Experiment 1 (Exp-1) with no puddling (P0); (b) EC_a (mS m^{-1}) of Experiment 2 (Exp-2) with Exp-2P1 (one puddling), Exp-2P2 (two puddling) and Exp-2P3 (three puddling); and (c) EC_a (mS m^{-1}) of Experiment 3 (Exp-3) with Exp-3P2 (two puddling), Exp-3P4 (four puddling), and Exp-3P6 (six puddling). The map coordinates are expressed in meters and conform to the Bangladesh Transverse Mercator projection with map datum Gulshan 303.

Flooding of non-saline paddy fields provides homogeneous soil water conditions because of water saturation. Under this condition and low values of OM content variation, a key role in influencing EC_a measurements is played by soil texture and bulk density (Rhoades et al., 1999; Saey et al., 2009b). Characterization of the field in terms of texture already indicated a limited spatial variability within the field. Besides, given that texture is a stable soil property which does not change laterally by puddling, the spatial distribution of EC_a of the three puddling areas is due to the spatial variation of plow pan compaction linked to soil bulk density variation (McKenzie et al., 2003). Higher bulk density variation of the soil resulted from puddling variation (different puddling intensity). Thus, more intensive puddling gave rise to higher bulk density values, especially in the compacted soil layer (0.15–0.30 m). Puddling of a soil results in redistribution of pore size with a pore geometry which is different than the soil in unpuddled condition. However, explaining the developmental mechanism of compaction and soil pore redistribution was beyond the scope of this research and can be found elsewhere (Kukal and Aggarwal, 2003; Kukal and Sidhu, 2004). In the plow pan layer, soil particles come into a closer state of contact and the layer is dominated by finer pores. The greater the connectivity and proportion of these fine pores, the larger the electrical conductivity becomes. Finer pore size plays a key role to increase the ion and electrolyte concentration within the pores which further influences the soil electrical conductance pathway (Brevik and Fenton, 2004).

Water Percolation

Puddling is required to maintain a wet growing condition for the paddy crop by decreasing water loss through percolation beyond the rooting zone. Therefore, measurements on water loss were taken to interpret the effectiveness of puddling intensities of Exp-2 and Exp-3. The statistical parameters of the 54 percolation measurements are given in Table 4.

A statistical comparison of the mean values grouped according to puddling intensities shows that a significantly higher mean percolation rate (37 mm d^{-1}) was found in Exp-2P1 where the intensity of puddling was relatively low. Increased puddling resulted in a significant decrease of percolation loss in Exp-3P4 (17 mm d^{-1}). Further increase in Exp-3P6 did not significantly decrease the percolation rate (16 mm d^{-1}) of water. Since Exp-2P2 and Exp-3P2 had larger mean water percolation values than Exp-3P4 and Exp-3P6, it can be reasonably accepted that a well-formed plow pan layer was not present there to restrict water losses through percolation. In sandy loam paddy field soils, Kukal and Aggarwal (2003) observed the percolation rate to be 30.1, 13.6, and 11.6 mm d^{-1} under unpuddled, medium, and high puddling intensity respectively, which is similar to the values found in this study. Soil particles in a closer state of contact within the compacted layer results in a sealing and thereby reduces the downward flow of water.

Paddy Rice Yield

The ultimate goal of puddling as a land preparation practice is to achieve optimal paddy rice productivity. Therefore, paddy yield data from 54 locations within the field were recorded for Exp-1 and Exp-3. The data were grouped according to the experimental treatments to allow yield comparison. The significance of the differences between the groups was analyzed statistically and is presented in Table 5.

The mean paddy yield was the lowest (5.7 Mg ha^{-1}) in P0 (Exp-1) when the field did not receive any puddling. Yield increased with an increase in puddling. The mean paddy yield was 5.8 Mg ha^{-1} in Exp-3P2 and increased significantly to 6.9 Mg ha^{-1} in Exp-3P4. This yield improvement of 1.1 Mg ha^{-1} is considerable given the smaller areas of the field receiving the puddling treatments. In Exp-3P6, no significant increase in paddy yield (mean = 7.0 Mg ha^{-1}) over Exp-3P4 was observed because water and nutrients were not limiting. However, the variation in yield was noticeably reduced (SD = 0.35 and 0.18 Mg ha^{-1} for Exp-3P4 and Exp-3P6, respectively). This is also indicated by an opposite trend of SD values with increased puddling from Exp-3P2 to Exp-3P6. This finding indicated the yield stabilization in Exp-3P4 for the given soil and crop type.

CONCLUSIONS

We puddled an inundated paddy rice field at varying intensities and characterized the puddled areas in terms of soil properties and EC_a. Detailed soil EC_a measured by an EMI based floating sensing system is able to clearly differentiate the variably compacted areas as the measured EC_a values increase with increasing soil compaction. Differences in soil bulk density and penetration resistance represent the compaction variability. The agronomic consequence of compaction can be evaluated using water percolation and paddy rice yield observations.

The EC_a map of a puddled paddy field clearly indicates the areas where more puddling is recommended to increase soil compaction. This information can effectively help the paddy grower to adjust tillage operation in advance of planting. The findings of this study also indicated that future research should be focused on exploring the relationship between changes in EC_a as influenced by a change in bulk density across larger paddy fields having a wider range of soil textural variation.

Table 4. Statistical parameters and mean comparison of water percolation rate (mm d^{-1}) stratified per puddling intensity treatment of Experiment 2 (Exp-2): Exp-2P1 = one puddling, Exp-2P2 = two puddling and Exp-2P3 = three puddling; Experiment 3 (Exp-3): Exp-3P2 = two puddling, Exp-3P4 = four puddling and Exp-3P6 = six puddling; *n* = number of samples per EC_a class, SD = standard deviation.

		Percolation rate (mm d^{-1})			
Puddling intensity	*n*	Minimum	Maximum	Mean†	SD
Exp-2P1	18	31	41	37_a	2.8
Exp-2P2	18	22	32	27_b	2.6
Exp-2P3	18	20	29	23_c	2.1
Exp-3P2	18	22	31	27_b	2.6
Exp-3P4	18	15	22	17_d	1.9
Exp-3P6	18	14	20	16_d	1.8

†Means followed by the same letter do not differ significantly (p = 0.05) according to Fisher's least significant difference test.

It was concluded that the EMI-based approach supports the evaluation of compaction variation during puddling. The sensing system appears to be a useful tool for precise land preparation and better resource utilization in paddy rice fields.

Table 5. Descriptive statistics and mean comparison of the paddy yield observations (Mg ha^{-1}) stratified per puddling intensity of Experiment 1 (Exp-1): P0 = no puddling and Experiment 3 (Exp-3): Exp-3P2 = two puddling, Exp-3P4 = four puddling and Exp-3P6 = six puddling.

	Harvest	Yield (Mg ha^{-1})				
Puddling intensity	year	*n*	Minimum	Maximum	Mean*	SD
P0 (Whole field)	2010	54	4.4	6.4	5.7_a	0.50
Exp-3P2	2011	18	4.8	6.5	5.8_a	0.59
Exp-3P4		18	6.0	7.5	6.9_b	0.35
Exp-3P6		18	6.7	7.3	7.0_b	0.18

*means followed by the same letter do not differ significantly (p = 0.05) according to Fisher's least significant difference test.

REFERENCES

Brammer, H. 1981. Reconnaissance soil survey of Dhaka District. Revised ed. Soil Resources Develop. Inst., Dhaka, Bangladesh. p. 6–19.

Brammer, H. 1996. The geography of the soils of Bangladesh. The Univ. Press Limited, Dhaka 1000, Bangladesh.

Brevik, E.C., and T.E. Fenton. 2004. The effect of changes in bulk density on soil electrical conductivity as measured with the Geonics EM-38. Soil Surv. Horiz. 45:96–102.

Brevik, E.C., T.E. Fenton, and A. Lazari. 2006. Soil electrical conductivity as a function of soil water content and implications for soil mapping. Precis. Agric. 7:393–404. doi:10.1007/s11119-006-9021-x

De Datta, S.K. 1981. Principles and practices of rice production. Wiley-Interscience, New York.

Gajri, P.R., K.S. Gill, R. Singh, and B.S. Gill. 1999. Effect of pre-planting tillage on crop yields and weed biomass in a rice–wheat system on a sandy loam soil in Punjab. Soil Tillage Res. 52:83–89. doi:10.1016/S0167-1987(99)00060-4

Goovaerts, P. 1997. Geostatistics for natural resources evaluation. Oxford Univ. Press, New York.

Hemmat, A., and V.I. Adamchuk. 2008. Sensor systems for measuring soil compaction: Review and analysis. Comput. Electron. Agric. 63:89–103. doi:10.1016/j.compag.2008.03.001

International Seed Testing Association. 2011. International rules for seed testing. International Seed Testing Association, Basserdorf, Switzerland.

Islam, M.M., and M. Van Meirvenne. 2011. FloSSy: A floating sensing system to evaluate soil variability of flooded paddy fields. In: J.V Stafford, editor, Proceedings of the 8th European conference on precision agriculture, Univ. of Life Sciences, Prague, Czech Republic. p. 60-66.

Islam, M.M., T. Saey, E. Meerschman, P. De Smedt, F. Meeuws, E. Van De Vijver, and M. Van Meirvenne. 2011. Delineating water management zones in a paddy rice field using a floating soil sensing system. Agric. Water Manage. 102:8–12. doi:10.1016/j.agwat.2011.10.001

Islam, M.M., E. Meerschman, T. Saey, P. De Smedt, E. Van De Vijver, and M. Van Meirvenne. 2012. Comparing apparent electrical conductivity measurements on a paddy field under flooded and drained conditions. Precis. Agric. 13:384–392. doi:10.1007/s11119-011-9253-2

Kukal, S.S., and G.C. Aggarwal. 2003. Puddling depth and intensity effects in rice–wheat system on a sandy loam soil. I. Development of subsurface compaction. Soil Tillage Res. 72:1–8. doi:10.1016/S0167-1987(03)00093-X

Kukal, S.S., and A.S. Sidhu. 2004. Percolation losses of water in relation to pre-puddling tillage and puddling intensity in a puddled sandy loam rice (*Oryza sativa*) field. Soil Tillage Res. 78:1–8. doi:10.1016/j.still.2003.12.010

McDonald, A.J., S.J. Riha, J.M. Duxbury, T.S. Steenhuis, and J.G. Lauren. 2006. Soil physical responses to novel rice cultural practices in the rice-wheat system: Comparative evidence from a swelling soil in Nepal. Soil Tillage Res. 86:163–175. doi:10.1016/j.still.2005.02.005

McNeill, J.D. 1980. Electromagnetic terrain conductivity measurement at low induction numbers. Tech. Note TN-6. Geonics Limited, Missisauga, ON, Canada.

McKenzie, N., R. Bramley, T. Farmer, L. Janik, W. Murray, C. Smith, and C. McLaughlin. 2003. Rapid soil measurement—A review of potential benefits and opportunities for the Australian grains industry. Client report for the Grains Research & Development Corporation, GRDC Contract No: CSO00027. GRDC/CSIRO Land and Water, Canberra, Australia.

Meul, M., and M. Van Meirvenne. 2003. Kriging soil texture under different types of nonstationarity. Geoderma 112:217–233. doi:10.1016/S0016-7061(02)00308-7

Mohanty, M., D.K. Painuli, and K.G. Mandal. 2004. Effect of puddling intensity on temporal variation in soil physical conditions and yield of rice (*Oryza sativa* L.) in a Vertisol. Soil Tillage Res. 76:83–94. doi:10.1016/j.still.2003.08.006

Mousavi, S.F., S. Yousefi–Moghadam, B. Mostafazadeh-Fard, A. Hemmat, and R. Yazdani. 2009. Effect of puddling intensity on physical properties of a silty clay soil under laboratory and field conditions. Paddy Water Environ. 7:45–54. doi:10.1007/s10333-008-0148-4

Playán, E., O. Pérez-Coveta, A. Martínez-Cob, J. Herrero, P. García-Navarro, B. Latorre, P. Brufau, and J. Garcés. 2008. Overland water and salt flows in a set of rice paddies. Agric. Water Manage. 95:645–658. doi:10.1016/j.agwat.2008.01.012

Rhoades, J.D., F. Chanduvi, and S.M. Lesch. 1999. Soil salinity assessment: Methods and interpretation of electrical conductivity measurements. FAO Rep. 57. FAO, Rome, Italy.

Saey, T., D. Simpson, H. Vermeersch, L. Cockx, and M. Van Meirvenne. 2009a. Comparing the EM38DD and DUALEM-21S sensors for depth-to-clay mapping. Soil Sci. Soc. Am. J. 73:7–12. doi:10.2136/sssaj2008.0079

Saey, T., M. Van Meirvenne, H. Vermeersch, N. Ameloot, and L. Cockx. 2009b. A pedotransfer function to evaluate the soil profile textural heterogeneity using proximally sensed apparent electrical conductivity. Geoderma 150:389–395. doi:10.1016/j.geoderma.2009.02.024

Sharma, P.K., and S.K. De Datta. 1985. Puddling influence on soil, rice development and yield. Soil Sci. Soc. Am. J. 49:1451–1457. doi:10.2136/sssaj1985.03615995004900060024x

Sheets, K.R., and J.M.H. Hendrickx. 1995. Non-invasive soil water content measurement using electromagnetic induction. Water Resour. Res. 31:2401–2409. doi:10.1029/95WR01949

Sudduth, K.A., J.W. Hummel, and S.J. Birrell. 1997. Sensors for site-specific management. In: F.J. Pierce and E.J. Sadler, editors, The state of site-specific management for agriculture. ASA, CSSA, and SSSA, Madison, WI. p. 183-210.

Walkley, A. and I.A. Black. 1934. An examination of Deftjareff method for determining soil organic matter and a proposed modifiction of the chromic acid titration method. Soil Sci. 37:29–37.

Webster, R., and M.A. Oliver. 2007. Geostatistics for environmental scientists. 2nd ed. John Wiley & Sons, Chichester.